Modeling and Optimization of Heat Transfer in Buckypaper Reinforced Polymer Composite

Aying Zhang[1,2,*], Haibao Lu[2,*], Yong Qing Fu[3], Zhenghong Li[2]

[1]Harbin University, Harbin 150086, PR China.

[2]Harbin Institute of Technology, Harbin 150001, PR China.

[3]Facultuy of Engineering and Environment, University of Northumbria, Newcastle upon Tyne, NE1 8ST, UK.

* Corresponding author. Tel./Fax: ＋86 451 86637951.

E-mail address: zaying@sina.com (A.Y. ZHANG)

luhb@hit.edu.cn (H.B. LU).

ABSTRACT

A heat transfer model of polymer composite reinforced by buckypaper was established in this study to analyze how the shapes, heating power and thermal conductivity of polymer matrix affect the temperature distribution and heating uniformity. Thermal responses of the polymer composites reinforced by flat and pulse bending buckypaper were systematically studied and the heating mechanisms of multiple-field coupling were investigated. The shapes and dimensions of the buckypaper are crucial in the optimization of such the polymer composites for heat generation. Results showed that the polymer composites reinforced by the flat buckypaper had relatively higher maximum and average temperature in a steady heated state compared with those by the pulse bending ones, whereas the minimum temperature of the composites reinforced by the flat buckypaper were relatively lower, so the temperature distribution in those flat ones was more non-uniform. The overall heating temperature of the polymer composites reinforced by both the flat and pulse bending buckypaper was increased linearly with the applied power. The larger the thermal conductivity of the polymer is, the lower the maximum and average temperature are.

Keywords: composites; buckypaper; finite element simulation; thermal conductivity; simulation analysis

INTRODUCTION

Carbon nanotubes (CNTs) have exceptionally good mechanical properties and thermal conductivity [1-4]. Experimental measurements of thermal conductivity (k_T) of individual CNTs revealed exceptionally good values at room temperature, which is ranging from 1400 W/(m•K) to 3000 W/(m•K) for multi-walled CNTs [5-8]. Single-walled CNTs (SWCNTs) have even higher thermal conductivity values [7,9] more than 6000 W/mK [10,11], which is much higher than those of the widely used copper and diamond. CNTs have other advantages beneficial for practical applications, including low thermal expansion coefficient, high chemical stability, and corrosion resistance to many

severe environments. As a result, CNTs were frequently mixed with polymers to enhance their thermal conducting performance [12,13]. Hu et al. reported that the thermal conductivity of silicon grease was enhanced by 70% after being mixed with 3 vol % multiwalled CNTs (MWCNTs) [14]. CNTs have also been recognized as a potential superior reinforcement agent for high-performance, multifunctional composites [15]. However, manufacturing CNT-reinforced composites with uniform tube dispersion and large CNT loading is a great challenge since the CNTs have a strong tendency to form bundles or ropes and rapidly increase the viscosity during processing [16]. Common problems such as non-uniform CNT dispersion within the polymer matrix, lack of adequate adhesion between the constituents of the composites, and nanotube mis-alignment have hindered significant improvements in CNT composite performance [15].

CNT-buckypaper based composites can overcome part of the above-mentioned critical issues, with advantages of high CNT content, good CNT orientation, and longer CNTs [17]. CNT buckypaper, the membrane materials composed of CNT network, are self-supporting networks of entangled CNT assemblies arranged in a random fashion and held together by van der Waals interactions at the tube-tube junctions [18-21]. Generally speaking, the exceptionally high thermal conductivity of individual CNTs does not guarantee high thermal conductivities for most of CNT materials, such as CNT films, mats, buckypaper, and vertically aligned arrays, which exhibit fairly small thermal conductivity in the range of 10-220 W/(m•K) [22-25]. However, buckypaper based composites can achieve a much higher concentration of CNTs and high conductive tube networks to maximize the electrical conductivity and mechanical properties [26]. Chen et al [27] reported that the heat conduction in a buckypaper depends greatly on CNT network formation. The buckypaper composed of multiwalled CNTs with large diameter (around 50 nm) and suitable length (1-10 μm) shows lower thermal impedance compared with those made by longer CNTs with smaller diameter. The thermal impedance of such buckypapers can be reduced to 0.27 $cm^2 \cdot K/W$, lower than that of commercialized graphite foil and thermal grease. Thus, the buckypaper may serve as a promising candidate for advanced thermal interface materials. Chen et al also indicated that the three-dimensional networks of buckypapers, with CNT orientations perpendicular to the surfaces, result in both the reduction of thermal contact resistance and the enhancement of heat conduction along the thickness. Endo et al [21] indicated CNT buckypaper may exhibit better thermal conducting performance not only in the plane but more importantly along the thickness direction compared with graphite films. CNT buckypaper has been considered as a competitive candidate for high-performance TIMs.

The buckypaper and its reinforced polymer composite materials have potential functions of fire proof, lightening protection and electromagnetic interference shielding. Effective integrating the buckypaper within novel materials could result in new types of sensors and functional materials. Shape-memory polymer (SMP) is one type of polymer material with a shape memory effect, i.e., with

an ability to return back to pre-deformed shape after responding to a particular stimulus. As one of the most popular actively moving materials, SMPs have many advantages, including low cost, light weight, a wide range of activation temperature (for heating-responsive shape recovery), high durability and high recoverable strain, which currently attract great research interest [28,29]. We have seen promising developments in many engineering applications, ranging from aerospace engineering to biomedical engineering [30]. Electrically conductive nanocomposite materials made of thermosensitive and buckypaper sheets not only have an excellent electrical conductivity, but also have a shape memory effect. Upon applying electricity, buckypaper produce resistance heating inside the polymer. When the temperature reaches the shape memory transformation temperature, the shape memory effect is triggered, and this is the principle for the electroactive SMP-based composites reinforced by the buckypaper. Lu et al [31] investigated the synergistic effect of self-assembled carbon nanofiber (CNF) nanopaper and the multi-layered interface on the electrical properties and electro-activated recovery behavior of shape memory polymer (SMP) nanocomposites. Results showed that the self-assembled multi-layered CNF nanopapers resulted in improved electrical conductivity and temperature distribution in the SMP nanocomposites. This design not only significantly enhances the reliability of bonding between the nanopaper and the SMP, resulting in an improved recovery ratio, but also provides a high speed electrical actuation.

In order to improve the actuation efficiency and optimize the structure of the buckypaper and SMP-based composites, the buckypaper's geometry and physical parameters on the thermal conductivity of SMP-based composites should be analyzed in order to provide a guide for application of the SMP-based composites reinforced by electric-driven buckypaper. However, the experimental work is limited by many random factors such as experimental errors and discreteness. Furthermore, once the geometry of the buckypaper is changed, lots of repetitive experiments have to be done in order to obtain the composites' new thermal properties. CNTs are relatively expensive and such repetitive work could consume enormous amount of raw materials. Therefore, it is important to design mathematical or simulation models to predict the thermal property of the buckypaper reinforced composite.

Previous research on the properties of buckypaper and buckypaper/polymer composites has mostly been concentrated on their mechanical properties and conductive properties. The studies on their thermal properties are less frequently reported, particularly for the thermal properties of buckypaper reinforced polymer composites analyzed by using an finite element softwares (FEA).

In this work, a heating model of the polymer composite reinforced by the buckypaper was established using a FEA software, FLUENT, and effects of the pulse bending shapes, heating power and thermal conductivity of the polymer matrix on the temperature distribution and heating uniformity were studied. The thermal responses of the polymer composites reinforced by flat and

pulse bending buckypaper were systematically studied and the heating mechanisms of multiple-field coupling were identified.

NUMERICAL MODELING

The heating model of the polymer composite reinforced by buckypaper is shown in Figure 1. The schematic diagram of the heating structure shows that the polymer matrix is heated by the buckypaper when the buckypaper is applied to an electrical source. In Figure 1, the buckypaper is driven by a power source, and the cube region is the polymer matrix which is heated by the buckypaper. T, L and w are the thickness, length and width of the polymer matrix, and h, d and A are the pulse bending height, thickness and pulse bending period of the buckypaper. The length, width, and the thickness of the heating model of the polymer composite reinforced by the flat and pulse bending buckypaper are 36 mm, 5 mm, 10 mm, and respectively. The thickness of the flat and pulse bending buckypaper is 0.8 mm. The pulse bending height and pulse bending period of the pulse bending buckypaper are 6 mm and 12 mm.

In the heating process, the polymer composite reinforced by buckypaper is static in the air, and convection is conducted between air and the composite surface. Assuming that the polymer matrix, buckypaper and ambient air temperature are in a state of thermal equilibrium in initially, the temperature of the polymer matrix is increased by the buckypaper when the buckypaper is electrically heated. Through the natural convection heat transfer with the environment, the composite material will reach a thermal stable state after a certain period of time.

The heat transfer by the buckypaper in the polymer matrix and the convection heat transfer between the outer surface of the polymer matrix and the external environment will be in a dynamic equilibrium process after the buckypaper is heated for a period of time with a stable power, which will reach to a stable temperature distribution of the composite material. The numerical simulation of the heating process was carried out mainly considered the natural convection due to temperature difference between the outer surface of the polymer matrix and the external environment, on the other hand, the conduction of heat generated from buckypaper after electrify inside the polymer matrix. Effects of the shapes, the heating power and the thermal conductivity of the polymer matrix on the temperature distribution and heating uniformity of the polymer composites reinforced by pulse bending and flat buckypaper were investigated using finite element software FLUENT. Comparative analysis was carried out for the following aspects:

(1) the shapes of buckypaper reinforcement: flat and pulse bending;

(2) the heating powers: 0.2 W, 0.3 W, 0.4 W, 0.6 W, 0.8 W, 1 W;

(3) the thermal conductivities of the polymer matrix: 0.10 W/(m•K), 0.15 W/(m•K), 0.20 W/(m•K), 0.25 W/(m•K).

Geometry Modeling

3D modeling software PROE 5 was used to establish the geometry model as shown in Figure 2 and Figure 3. The grid work is done by software ICEM, the total number of grids is about 480,000. Blocking is chosen as the element type. The grid is then exported to the software FLUENT.

Figure 2 shows the geometry model of the polymer composite reinforced by the pulse bending buckypaper. The length, width and the height of the model are 36 mm, 5 mm, 10 mm. The pulse bending period, pulse bending height, width and thickness of the pulse bending buckypaper are 12 mm, 6 mm, 5 mm, 0.8 mm. As shown in Figure 2, the purple red part is the pulse bending buckypaper, and the blue part is the polymer matrix.

Figure 3 shows the geometric model of the polymer composite reinforced by the flat buckypaper. The length, width and height of the model are 36 mm, 5 mm, 10 mm. The thickness of the pulse bending buckypaper is 0.8 mm. As shown in Figure 3, the purple red part is the flat buckypaper, and the blue part is the polymer matrix.

Calculation Condition

The external boundary is set to third kinds of boundary conditions. Assuming that the electric heating power is converted into internal energy and the heat source per unit volume is equal to the ratio of heating power to its volume. The natural convection heat transfer coefficient was set to be 10 W/(m^2•K). The ambient temperature was set to be 300 K. The thermal conductivity of the buckypaper and the polymer matrix was set to be 1.5 W/(m•K) and 0.2 W/(m•K), respectively. The specific heat capacity of the buckypaper and the polymer matrix was set to be 800 J/(kg•K) and 1000 J/(kg•K), respectively. The densities of the buckypaper and the polymer matrix were set to be 0.3 g/cm^3 and 1.2 g/cm^3, respectively.

RESULTS AND DISCUSSION

Steady State Result Analysis

Influence of Shape of Buckypaper Heating Sheets

The inner heat source of the buckypaper heating sheets was calculated as functions of the ratio of heating power and volume of the buckypaper heating sheets. The thickness of the pulse bending and flat buckypaper was 0.8 mm, and the heating power was 0.3 W. The inner heat source of the buckypaper with pulse bending heating sheets can be obtained by formula (1).

$$q_{Vbent} = \frac{0.3\text{W}}{\left(0.8\times5\times22.4\times10^{-9}\right)\text{m}^3\times3} = 1116071\text{W/m}^3 \quad (1)$$

The inner heat source of the buckypaper with flat heating sheets can be obtained by formula (2).

$$q_{Vflat} = \frac{0.3\text{W}}{\left(0.8\times5\times36\times10^{-9}\right)\text{m}^3} = 2083333\text{W/m}^3 \quad (2)$$

The temperature of the polymer composites reinforced by different shape buckypaper at stable states along the section x=0 and z=0 in Figures 2 and 3 are listed in Table 1.

Compared to those from the polymer composites reinforced by the pulse bending buckypaper, the maximum and average temperature of the polymer composites reinforced by flat buckypaper at the stable states along the section x=0 and z=0 are relatively higher, and the minimum temperature obtained are relatively lower. Because the inner heat source of flat buckypaper heating sheets (q_{vflat}) is larger than that of pulse bending buckypaper heating sheets ($q_{vpulse\ bending}$) as shown in formula (1) and formula (2), the resulted heat generation from the flat buckypaper heating sheet is relatively higher. The temperature difference between the maximum and minimum temperature is linked with the temperature distribution inside the composites. Therefore, the results indicate that the uniformity of temperature distribution in the polymer composites reinforced by flat buckypaper is relatively poor. Non-uniform temperature distribution can lead to thermal stress in the composites, which degrade mechanical property of the composites.

The temperature distribution of the polymer composites reinforced by pulse bending and flat buckypaper at the stable states along the section z=0 were calculated. The obtained temperature distribution maps are shown in Figures 4 and Figures 5. Clearly, high temperature region appear in the vicinity of both pulse bending and flat buckypaper. Figure 4 shows that heat transfer of pulse bending buckypaper could occur in both vertical and horizontal directions due to the presence of heating sheets in the vertical direction, which results in that high temperature region is larger than that of flat buckypaper. The temperature distribution uniformity has been improved because heat conduction region of the pulse bending buckypaper in the polymer matrix is larger than that of flat buckypaper.

Influence of Heating Power

The temperature distributions of the polymer composites reinforced by pulse bending and flat buckypaper at stable states along the section z=0 were analyzed under different heating powers of 0.2 W, 0.3 W, 0.4 W, 0.6 W, 0.8 W and 1 W. The other parameters of the calculation model are the same. The obtained maximum, minimum and average temperature of the composites under different heating powers is listed in Table 2.

Table 2 lists that the maximum, minimum and average temperature of the composites was increased as the heating power were increased from 0.2 to 1.0 W, and so was the temperature difference between the maximum and minimum temperature. Because the total volume of pulse bending buckypaper is slightly larger than that of the flat buckypaper under the calculation conditions, the inner heat source of flat buckypaper heating sheets is larger than that of pulse bending buckypaper heating sheets under the same heating power as shown in formula (1) and (2). The larger the inner heat source of flat buckypaper is, the higher the heat has been produced. Accordingly, the maximum, and average

temperature of the polymer composites reinforced by flat buckypaper at a stable state is higher than those of pulse bending buckypaper. Compared to the polymer composites reinforced by the flat buckypaper, the minimum temperature of the polymer composites reinforced by pulse bending buckypaper is higher when the heating power is increased to a same reading, whereas the temperature difference between the maximum and minimum temperature is lower, which indicates that the temperature distribution of the polymer composites reinforced by pulse bending buckypaper is more uniform.

The temperature distribution maps of the polymer composites reinforced by pulse bending and flat buckypaper along the section z=0 were obtained and the results are shown in Figures 6 and 7. The temperature distribution of the polymer composites reinforced by pulse bending and flat buckypaper becomes worse as the heating power is increased from 0.2 to 1.0 W.

The relationship between the temperature and heating power has also summarized in Figures 8 and 9, and the maximum, minimum and average temperature of the composites reinforced by pulse bending and flat buckypaper at stable states along the section z=0 increase linearly as the heating power is increased from 0.2 to 1.0 W.

Figure 10 shows that the heating rate of the polymer composites reinforced by flat buckypaper is slightly faster compared to those reinforced by pulse bending buckypaper as the heating power is increased from 0.2 to 1.0 W, due to the higher the inner heat source of flat buckypaper at the same heating power.

Table 3 lists the calculated thermal flows of the polymer composites on the external surface, and the results show an upward increase trend as the heating power is increased from 0.2 W to 1.0 W. The heating sheets of the pulse bending buckypaper presented in both vertical and horizontal direction, and thus result in the increased thermal flow of the polymer matrix embedded by pulse bending buckypaper on the external surface under the same heating power. The heat transfer of pulse bending buckypaper could happen from both vertical and horizontal directions, which result in that the temperature distribution is more uniform.

Influence of the Thermal Conductivity of Polymer Matrix

The temperature distribution of the polymer composites with various thermal conductivities of the polymer matrix along the section z=0 was analyzed. The thermal conductivity of the buckypaper was set to be 1.5 W/(m•K), and those of the polymer matrix were set to be s 0.10, 0.15, 0.20 and 0.25 W/(m•K). The other conditions of the calculation model were the same. Table 4 shows that the maximum and average temperature of the polymer composites are decreased as the thermal conductivity of polymer matrix is increased from 0.10 to 0.25 W/(m•K), whereas the minimum temperature show an increasing trend.

The heat transfer capability of polymer matrix is enhanced as its thermal conductivity is increased

from 0.10 to 0.25 W/(m•K), because the heat produced by the buckypaper is more easily transmitted through the polymer to the outer interface. The heat is not easily accumulated inside the polymer matrix, so the maximum and average temperature are decreased. The minimum temperature of the composites are increased as the thermal conductivity of the polymer matrix is increased, which results in a more uniform temperature distribution.

As shown in Figures 11 and 12, The temperature distribution maps indicate that the temperature become uniformly distributed when the thermal conductivity of the polymer matrix is increased from 0.10 to 0.25 W/(m•K).

Table 5 summarizes the calculated thermal flow of pulse bending and flat buckypaper. Results showed there is a decreasing trend, and the thermal flow of the polymer matrix along the external surface shows an upward trend as the thermal conductivity is increased from 0.10 to 0.25 W/(m•K).

CONCLUSION

The heat transfer model of the polymer composite reinforced by buckypaper was proposed and FLUENT simulation software was used to analyze how the pulse bending shapes, the heating power and the thermal conductivity of the polymer matrix affect the temperature distribution and heating uniformity.

Compared to the polymer composites reinforced by the pulse bending buckypaper, the ones reinforced by the flat buckypaper have relatively higher maximum and average temperature in the steady states, while the minimum temperature decreases. The heating rate of the average temperature with the flat buckypaper was much faster compared to the polymer composites reinforced by pulse bending buckypaper, but the temperature distribution is not uniform.

With the increase of heating power, the overall heating temperature is increased linearly when the composites reinforced by buckypaper reaches a steady state. This is due to the fact that the convection heat dissipation rate is not as high as the increasing rate of the heat production, and with the continuous heating, the heating rate generated form the materials decreases gradually.

The larger the thermal conductivity of the polymer is, the lower the maximum and average temperature are. As the minimum temperature is increased, the distribution of the temperature is more uniform. This is because with increase of the thermal conductivity of the polymer matrix, the heat generated from the buckypaper sheets is more uniformly distributed, and the heat will not be accumulated in the interior of the polymer matrix. Therefore, the maximum and average temperature is decreased. Meanwhile, the increased thermal conductivity of the polymer matrix leads to more uniform temperature distribution and increased lowest temperature.

Acknowledgement

This work was financially supported by Heilongjiang Natural Science Foundation (Grant No. E201454).

REFERENCES

[1] R. S. Ruoff, D. C. Lorents. Mechanical and thermal properties of carbon nanotubes [J]. Carbon, 1995, 33(7):925-930.

[2] J. Hone, J. E. Fischer. Quantized phonon spectrum of single-wall carbon nanotubes [J]. Science, 2000, 289(5485): 1730-1733.

[3] S. Berber, Y. K. Kwon, D. Tomanek. Unusually high thermal conductivity of carbon nanotubes [J]. Physical Review Letters, 2000, 84(20):4613-4616.

[4] M. A. Osman, D. Srivastava. Temperature dependence of the thermal conductivity of single-wall carbon nanotubes [J]. Nanotechnolgy, 2001, 12(1):21-24.

[5] P. Kim, L. Shi, A. Majumdar, P. L. McEuen. Thermal transport measurements of individual multiwalled nanotubes [J]. Physical Review Letters, 2001, 87(87):265-266.

[6] M. Fujii, X. Zhang, H. Xie, et al. Measuring the thermal conductivity of a single carbon nanotube [J]. Physical Review Letters, 2005, 95(6): 065502.

[7] Q. Li, C. Liu, X. Wang, et al. Measuring the thermal conductivity of individual carbon nanotubes by the Raman shift method [J]. Nanotechnology, 2009, 20(14):5886-5890.

[8] A. A. Balandin. Thermal properties of graphene and nanostructured carbon materials [J]. Nature Materials, 2011, 10(8): 569-581.

[9] E. Pop, D. Mann, Q. Wang, et al. Thermal conductance of an individual single-wall carbon nanotube above room temperature [J]. Nano Letter, 2005, 6(1): 96-100.

[10] C.Yu, L.Shi, Z.Yao, et al. Thermal Conductance and Thermopower of an Individual Single-Wall Carbon Nanotube [J]. Nano Letter, 2005, 5(9): 1842-1846.

[11] N. Mingo, D. A.Broido. [J]. Length Dependence of Carbon Nanotube Thermal Conductivity and the “Problem of Long Waves” [J]. Nano Letter, 2005, 5(7): 1221-1225.

[12] J. Park, M. T. Taya. Design of Thermal Interface Material With High Thermal Conductivity and Measurement Apparatus [J]. Journal of Electronic Packaging, 2006, 128(1): 46-52.

[13] Y. Xu, C. K. Leong, D. D. L. Chung. Carbon Nanotube Thermal Pastes for Improving Thermal Contacts [J]. Journal of Electronic Materials, 2007, 36(9): 1181-1187.

[14] X. Hu, L. Jiang, K. E. Goodson. Thermal conductance enhancement of particle-filled thermal interface materials using carbon nanotube inclusions [C]. Therm. Phenom.2004, 1: 63-69.

[15] C. Y. Chang, E. M. Phillips, R. Liang, et al. Alignment and Properties of Carbon Nanotube Buckypaper/Liquid Crystalline Polymer Composites [J]. Journal of Applied Polymer Science, 2013, 128(3): 1360-1368.

[16] Z. Wang, Z. Liang, B. Wang, et al. Processing and property investigation of single-walled carbon nanotube (SWNT) buckypaper/epoxy resin matrix nanocomposites [J]. Composites: Part A,

2004, 35(10):1225-1232.

[17] L. Song, H. Zhang, Z. Zhang, et al. Processing and performance improvements of SWNT paper reinforced PEEK nanocomposites [J]. Composites: Part A 2007; 38: 388-392.

[18] Z. Spitalsky, G. Tsoukleri, D. Tasis, et al. High volume fraction carbon nanotube-epoxy composites [J]. Nanotechnology, 2009, 20(40): 17579-17584.

[19] F. Giubileo, A. D. Bartolomeo, M. Sarno, et al. Field emission properties of as-grown multiwalled carbon nanotube films [J]. Carbon 2012, 50(1): 163-169.

[20] Q. Wu, C. Zhang, R. Liang, et al. Fire retardancy of a buckypaper membrane [J]. Carbon, 2008, 46(8): 1164-1165.

[21] M. Endo, H. Muramatsu, T. Hayashi, et al. Nanotechnology: 'buckypaper' from coaxial nanotubes [J]. Nature 2005, 433: 7025.

[22] J. Hone, M. C. Llaguno, N. M. Nemes, et al. Electrical and thermal transport properties of magnetically aligned single wall carbon nanotube films [J]. Applied Physics Letters. 2000, 77(8):1450-1452.

[23] P. Gonnet, Z. Liang, E. S. Choi, et al. Thermal conductivity of magnetically aligned carbon nanotube buckypaper and nanocomposites [J]. Current Applied Physics, 2006, 6(1):119-122.

[24] I. Ivanov, A. Puretzky, G. Eres, et al. Fast and highly anistropic thermal transport through vertically aligned carbon nanotube arrays [J]. Applied Physics Letters, 2006, 89(22): 223110-223113.

[25] M. E. Itkis, F. Borondics, A. Yu, et al. Thermal conductivity measurements of semitransparent single-walled carbon nanotube films by a bolometric technique [J]. Nano Letter. 2007, 7(4): 900-904.

[26] J. W. Zhang, D. Z. Jiang, H. X. Peng, et al. Enhanced mechanical and electrical properties of carbon nanotube buckypaper by in situ cross-linking [J]. Carbon, 2013, 63(2): 125-132.

[27] H. Y. Chen, M. H. Chen, J. T. Di, et al. Architecting Three-Dimensional Networks in Carbon Nanotube Buckypapers for Thermal Interface Materials [J]. The Journal of Physical Chemistry C, 2012, 116(6): 3903-3909.

[28] K. Gall, M. L. Dunn, Y. P. Liu, G. Stefanic. Internal Stress Storage in Shape Memory Polymer Nanocomposites [J]. Applied Physics Letters, 2004, 85(2): 290-292.

[29] I. Gurevitch, M. S. Silverstein. Shape memory polymer foams from emulsion templating [J]. Soft Matter, 2012, 8(8): 10378-10387.

[30] D. J. Maitland, M. F. Metzger, D. Schumann, et al. Photothermal properties of shape memory polymer micro-actuators for treating stroke [J]. Lasers in Surgery & Medicine, 2001, 30(1):1-11.

[31] H. B. Lu, F. Liang, J. H. Gou, et al. Synergistic effect of self-assembled carbon nanopaper and multi-layered interface on shape memory nanocomposite for high speed electrical actuation [J].

Journal of Applied Physics, 2014, 115(6): 064907-064907

Tables caption:

Table 1 Temperature of composites reinforced by pulse bending and flat buckypaper along the section x=0 and z=0

Table 2 Temperature of composites reinforced by pulse bending and flat buckypaper along the section z=0 under different heating powers

Table 3 Average thermal flow of the composites reinforced by pulse bending and flat buckypaper along external surface under different heating powers (W/m^2)

Table 4 Temperature of composites reinforced by pulse bending and flat buckypaper along the section z=0 under different thermal conductivities of polymer matrix

Table 5 Average thermal flow of the composites reinforced by pulse bending and flat buckypaper along external surface under different thermal conductivities (W/m^2)

Table 1 Temperature of composites reinforced by pulse bending and flat buckypaper along the sections x=0 and z=0

Heater/W	Section of x=0			Section of z=0		
	T_{max}/K	T_{min}/K	T_{ave}/K	T_{max}/K	T_{min}/K	T_{ave}/K
Pulse	330.71	323.35	327.99	330.90	319.95	327.57
Flat	335.61	323.32	329.23	335.61	319.71	328.32

Table 2 Temperature of composites reinforced by pulse bending and flat buckypaper along the section z=0 under different heating powers

Heating power	Pulse bending			Flat		
/W	T_{max}/K	T_{min}/K	T_{ave}/K	T_{max}/K	T_{min}/K	T_{ave}/K
0.2	320.57	313.28	318.35	323.66	313.10	318.82
0.3	330.91	319.95	327.57	335.62	319.71	328.32
0.4	341.12	326.59	336.72	347.44	326.26	337.73
0.6	361.72	339.90	355.10	371.19	339.40	356.61
0.8	382.24	353.18	373.43	394.89	352.52	375.47
1.0	402.83	366.49	391.81	418.56	365.61	394.29

Table 3 Average thermal flow of the composites reinforced by pulse bending and flat buckypaper along external surface under different heating powers (W/m^2)

Heating power	Pulse bending		Flat	
/W	Buckypaper	Polymer Matrix	Buckypaper	Polymer Matrix
0.2	191.62	166.87	221.45	165.96
0.3	287.88	250.70	333.28	249.76
0.4	383.42	333.91	443.98	332.73
0.6	575.38	501.08	666.15	499.24
0.8	766.81	667.79	888.01	665.52

1.0	958.76	834.95	1109.47	831.49

Table 4 Temperature of composites reinforced by pulse bending and flat buckypaper along the section z=0 under different thermal conductivities of polymer matrix

Thermal conductivity /W/(m•K)	Pulse bending			Flat		
	T_{max}/K	T_{min}/K	T_{ave}/K	T_{max}/K	T_{min}/K	T_{ave}/K
0.10	334.42	316.87	329.25	343.34	316.43	330.68
0.15	332.15	318.79	328.15	338.33	318.48	329.15
0.20	330.90	319.95	327.57	335.61	319.71	328.32
0.25	330.09	320.74	327.20	333.92	320.54	327.81

Table 5 Average thermal flow of the composites reinforced by pulse bending and flat buckypaper along external surface under different thermal conductivities (W/m^2)

Thermal conductivity /W/(m•K)	Pulse bending		Flat	
	Buckypaper	Polymer matrix	Buckypaper	Polymer matrix
0.10	404.58	245.44	318.64	247.31
0.15	358.02	248.34	298.43	249.55
0.20	333.28	249.76	287.88	250.70
0.25	318.08	250.74	281.38	251.36

Figures caption:

Figure 1. Sketch diagram of heating experimental device

Figure 2. Model of the polymer composites reinforced by pulse bending buckypaper

Figure 3. Model of the polymer composites reinforced by flat buckypaper

Figure 4. Temperature distribution maps of composites reinforced by pulse bending buckypaper along the section z=0

Figure 5. Temperature distribution maps of composites reinforced by flat buckypaper along the section z=0

Figure 6. Temperature distribution maps of composites reinforced by pulse bending buckypaper along the section z=0 under different heating powers

Figure 7. Temperature distribution maps of composites reinforced by flat buckypaper along the section z=0 under different heating powers

Figure 8. Temperature distribution of composites reinforced by pulse bending buckypaper along the section z=0 under different heating powers

Figure 9. Temperature distribution of composites reinforced by flat buckypaper along the section z=0 under different heating powers

Figure 10. Curve of average temperature of composites reinforced by pulse bending and flat buckypaper along the section z=0 under different heating powers

Figure 11. Temperature distribution maps of composites reinforced by pulse bending buckypaper along the section z=0 under different thermal conductivity of polymer matrix

Figure 12. Temperature distribution maps of composites reinforced by flat buckypaper along the

section z=0 under different thermal conductivity of polymer matrix

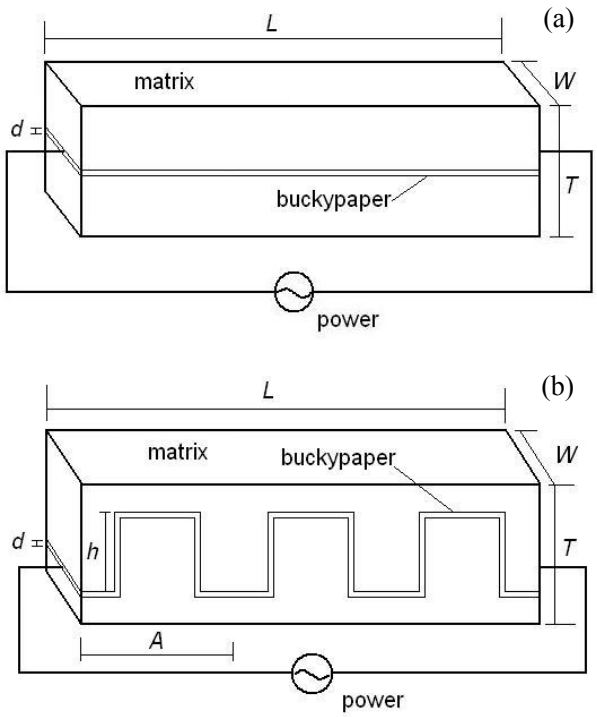

Fig. 1 Sketch diagram of heating experimental test of (a) flat buckpaper, (b) pulse bending buckypaper

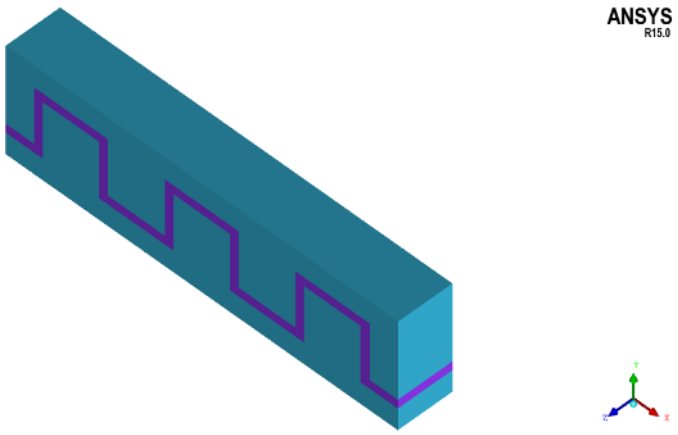

Fig. 2 Model of the polymer composites reinforced by pulse bending buckypaper

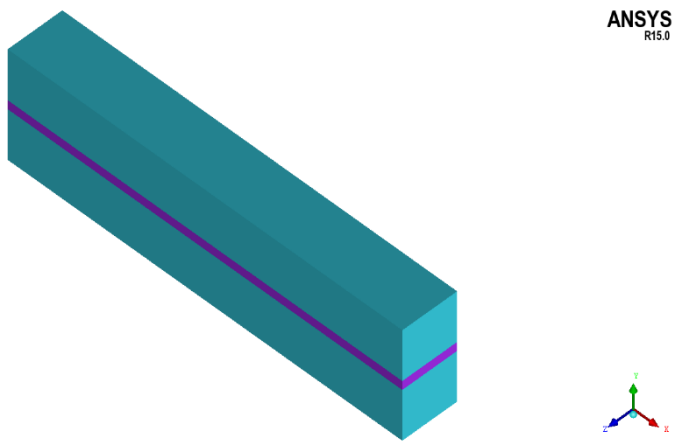

Fig. 3 Model of the polymer composites reinforced by flat buckypaper

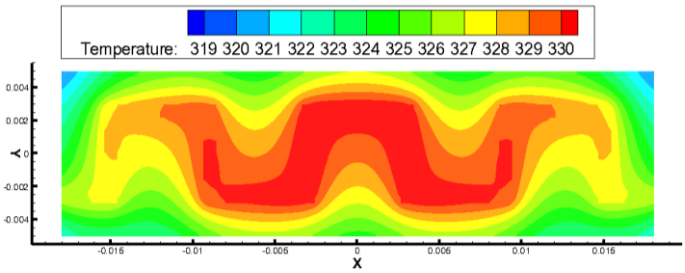

Fig. 4 Temperature distribution maps of composites reinforced by pulse bending buckypaper along the section z=0

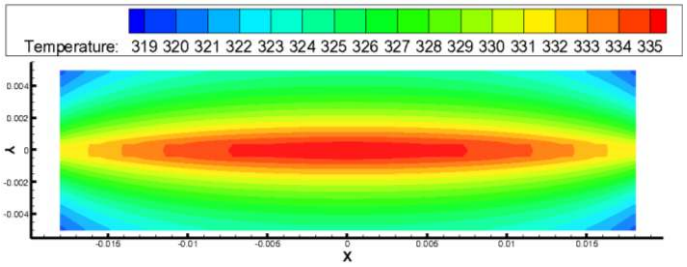

Fig.5 Temperature distribution maps of composites reinforced by flat buckypaper along the section z=0

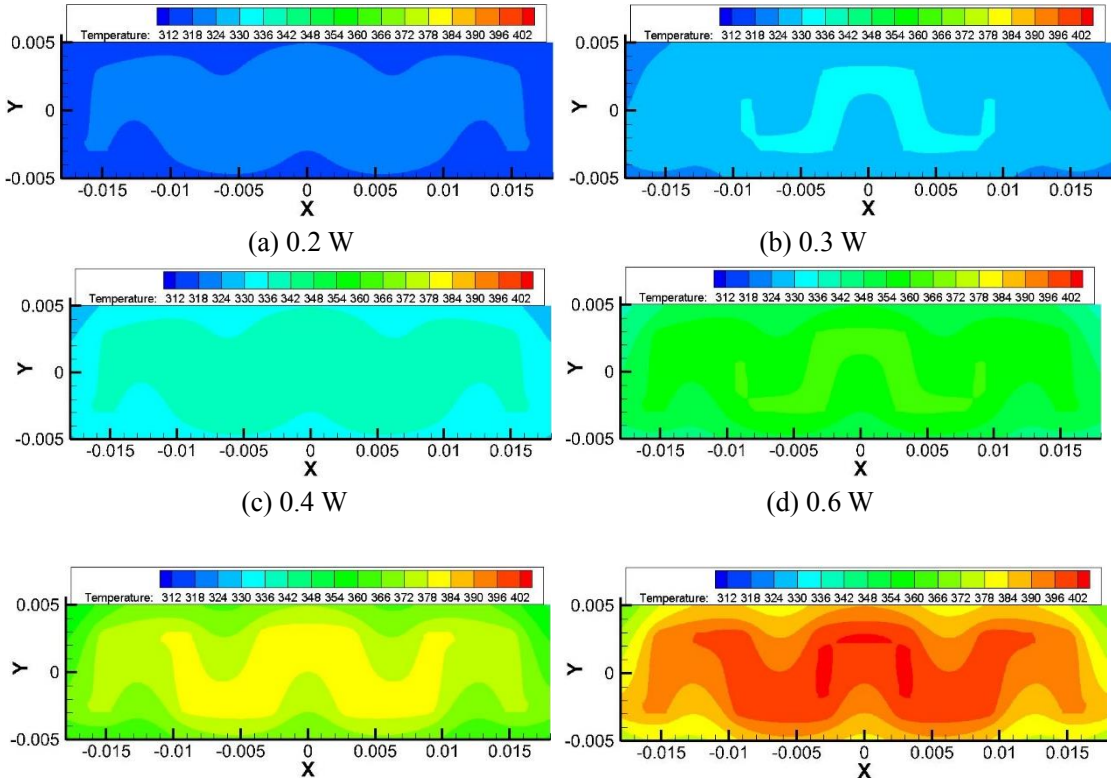

(a) 0.2 W (b) 0.3 W

(c) 0.4 W (d) 0.6 W

(e) 0.8 W (f) 1.0 W

Fig. 6 Temperature distribution maps of composites reinforced by pulse bending buckypaper along the section z=0 under different heating powers

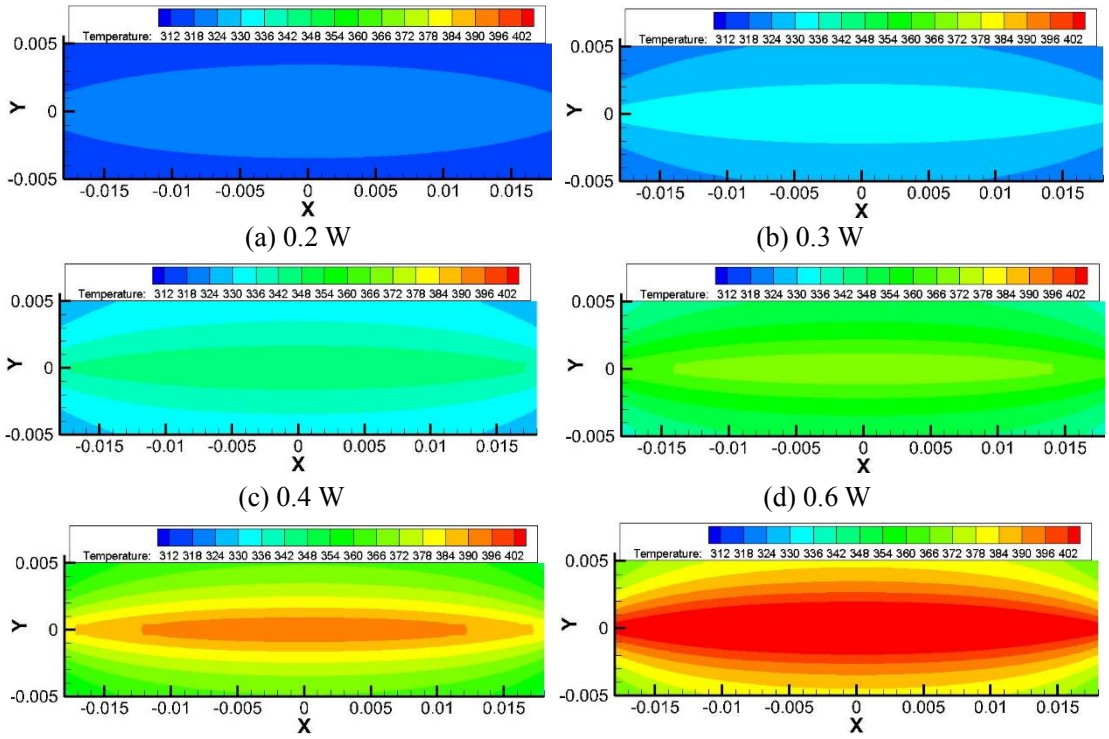

(a) 0.2 W (b) 0.3 W

(c) 0.4 W (d) 0.6 W

(e) 0.8 W (f) 1.0 W

Fig. 7 Temperature distribution maps of composites reinforced by flat buckypaper along the section z=0 under different heating powers

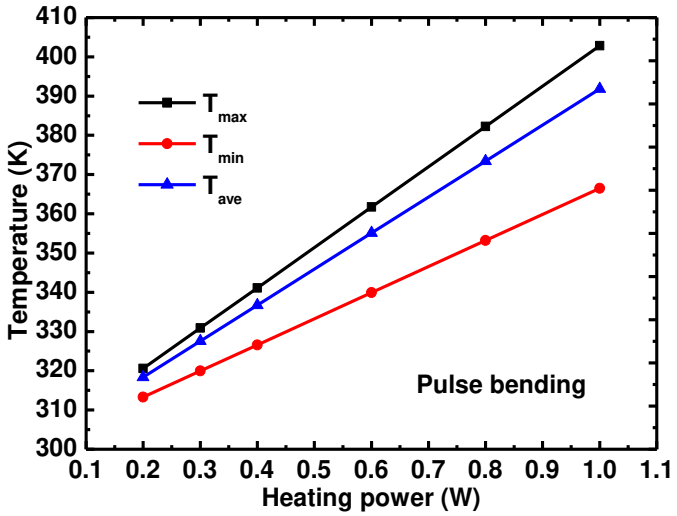

Fig. 8 Temperature distribution of composites reinforced by pulse bending buckypaper along the section z=0 under different heating powers

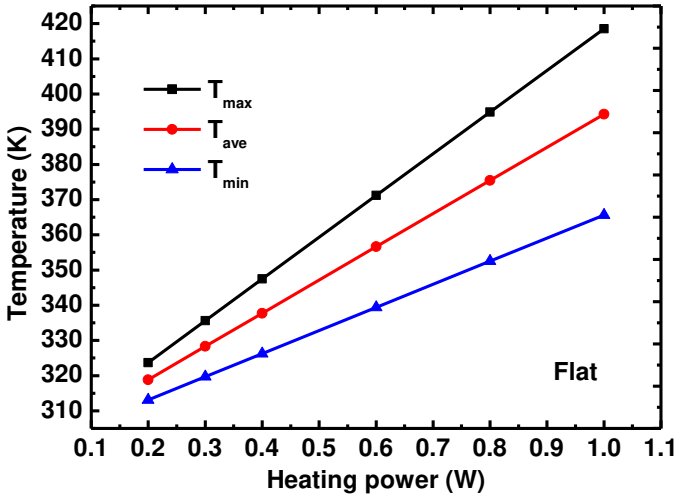

Fig. 9 Temperature distribution of composites reinforced by flat buckypaper along the section z=0 under different heating powers

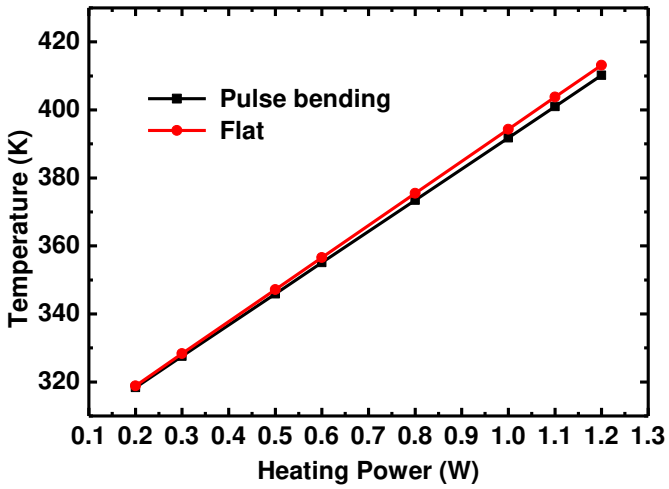

Fig.10 Curve of average temperature of composites reinforced by pulse bending and flat buckypaper along the section z=0 under different heating powers

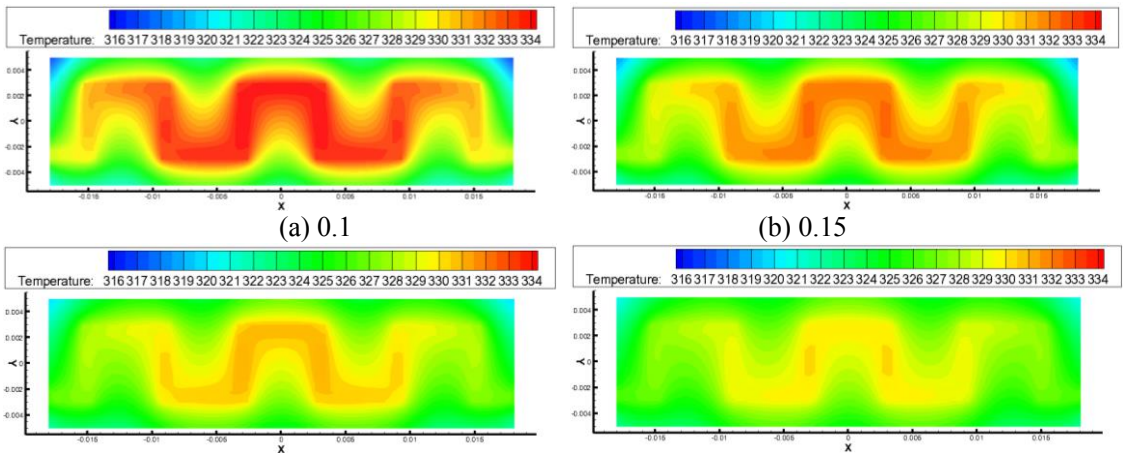

(a) 0.1 (b) 0.15

(c) 0.2 (d) 0.25

Fig.11 Temperature distribution maps of composites reinforced by pulse bending buckypaper along the section z=0 under different thermal conductivity of polymer matrix

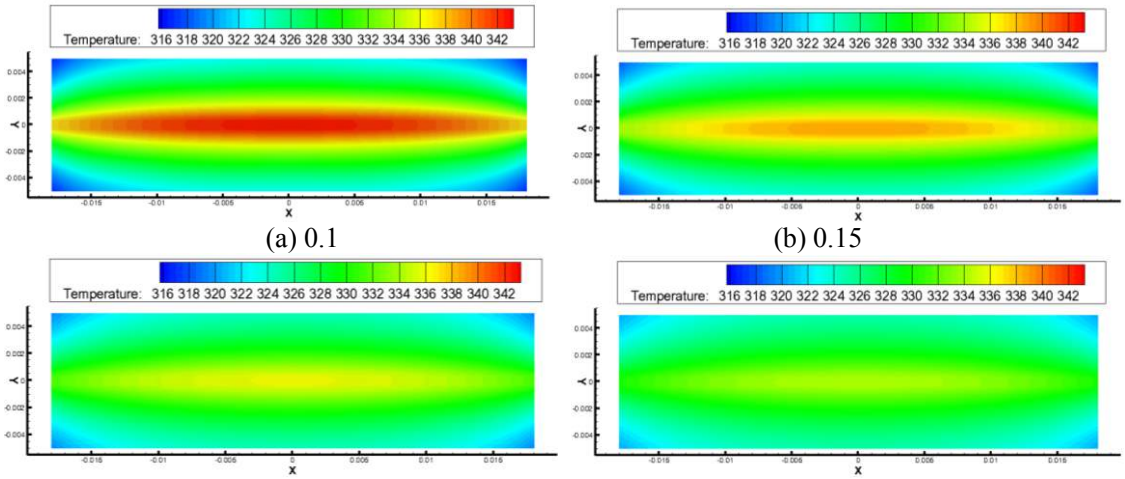

(a) 0.1 (b) 0.15

(c) 0.2 (d) 0.25

Fig.12 Temperature distribution maps of composites reinforced by flat buckypaper along the section z=0 under different thermal conductivity of polymer matrix